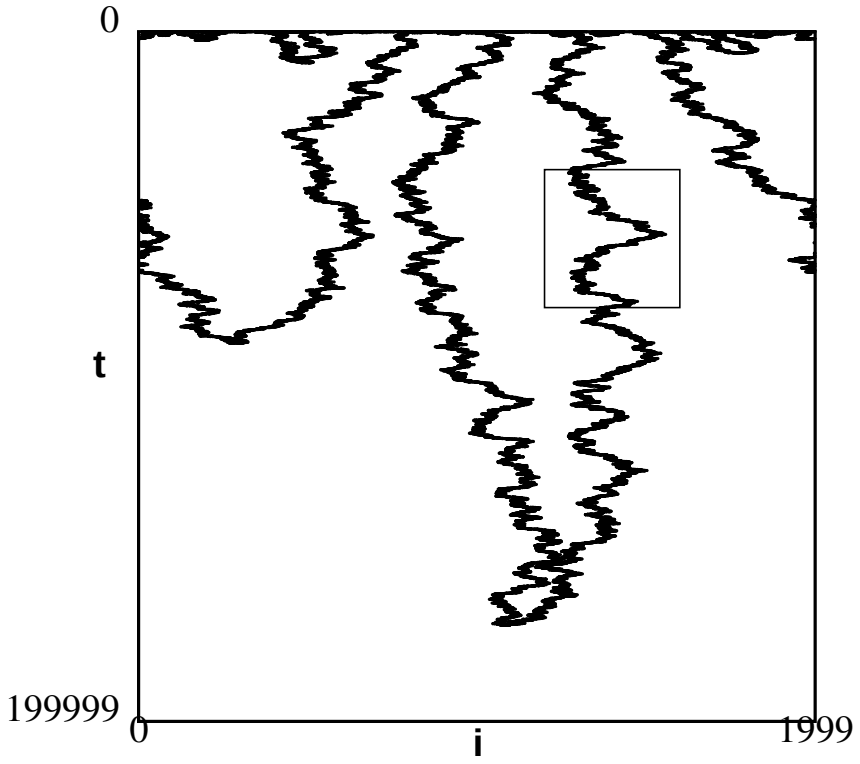

Fig. 10.23 Trajectories of dislocations evolving from a random initial configuration. The time and space scales are highly contracted to show the diffusive behavior. Every fifth iteration is displayed. The square indicates the region displayed in fig. 10.24.

gas on a very large lattice; that is, initial patterns with widely separated dislocations of the form $(\Sigma 0)^* 11 (0\Sigma)^*$. Additionally, dislocations after $t = 0$ were detected only as isolated pairs of 1s; i.e. as $(\Sigma 0)^* 11 (0\Sigma)^*$ again. Thus, dislocations were not counted in any other form, such as $(\Sigma 0)^* 10^{2n} 1 (0\Sigma)^*, n = 1, 2, \ldots$. The consequence is that statistics could only be gathered relatively infrequently and for a limited type of initial ensemble. Here we avoid these problems entirely and collect substantially better statistics on unrestricted initial conditions by using the machine metric of section 4.6 to estimate the dislocation number density

$$d_N(t) = N^{-1} \|\Phi_t(\mathbf{s})\|_{\mathrm{M}(\Lambda^0)} \tag{10.3}$$

We count the density $d_N(t)$ of dislocations at each time in a randomly-generated state $\mathrm{s} \in \mathcal{A}^N$. The result is shown in fig. 10.26, where we see $d_{10^5}(t)$ plotted against time. As the straight line suggests, we find $d(t) = \frac{1}{\sqrt{8\pi D}} t^{-\alpha}$ with least-squares analysis giving values of $D = 0.54$ and $\alpha = 0.49 \pm 0.04$. The estimate is from a fit over data at all times.

Motion of an isolated dislocation

At the beginning of this section, we noted that a single dislocation in ECA 18 performs a random walk. The proof of this, however, relies on a detailed analysis